

Changing nutrient stoichiometry affects phytoplankton production, DOP accumulation and dinitrogen fixation – a mesocosm experiment in the eastern tropical North Atlantic

Meyer, J.^{1*}, Löscher, C. R.^{1,2*}, Neulinger, S. C.², Reichel, A. F.¹, Loginova, A.¹, Borchard, C.¹, Schmitz, R. A.², Hauss, H.¹, Kiko, R.¹, Riebesell, U.^{1,3}

1 [1] GEOMAR Helmholtz Centre for Ocean Research Kiel, Düsternbrooker Weg 20, 24105 Kiel,
2 Germany

3 [2] Institute of General Microbiology, Christian-Albrechts-University Kiel, Am Botanischen Garten 1-9,
4 24118 Kiel, Germany

5 [3] Christian-Albrechts-University Kiel, Christian-Albrechts-Platz 4, 24118 Kiel, Germany

6 Correspondence to: jumeyer@geomar.de

* Authors contributed equally to this study

1 **Abstract:**

2 Ocean deoxygenation due to climate change may alter redox-sensitive nutrient cycles in the marine
3 environment. The productive eastern tropical North Atlantic (ETNA) upwelling region may be
4 particularly affected when the relatively moderate oxygen minimum zone (OMZ) deoxygenates further
5 and microbially-driven nitrogen (N) loss processes are promoted. Consequently, water masses with a
6 low nitrogen to phosphorus (N:P) ratio could reach the euphotic layer, possibly influencing primary
7 production in those waters. Previous mesocosm studies in the oligotrophic Atlantic Ocean identified
8 nitrate availability as a control of primary production, while a possible co-limitation of nitrate and
9 phosphate could not be ruled out. To better understand the impact of changing N:P ratios on primary
10 production and N₂ fixation in the ETNA surface ocean, we conducted land-based mesocosm
11 experiments with natural plankton communities and applied a broad range of N:P ratios (2.67 – 48).
12 Silicic acid was supplied at 15 μmol L⁻¹ in all mesocosms. We monitored nutrient drawdown, biomass
13 accumulation and nitrogen fixation in response to variable nutrient stoichiometry. Our results
14 confirmed nitrate to be the key factor determining primary production. We found that excess
15 phosphate was channeled through particulate organic matter (POP) into the dissolved organic matter
16 (DOP) pool. In mesocosms with low inorganic phosphate availability, DOP was utilized while N₂
17 fixation increased, suggesting a link between those two processes. Interestingly this observation was
18 most pronounced in mesocosms where nitrate was still available, indicating that bioavailable N does
19 not necessarily suppress N₂ fixation. We observed a shift from a mixed cyanobacteria/proteobacteria
20 dominated active diazotrophic community towards a diatom-diazotrophic association of the *Richelia*-
21 *Rhizosolenia* symbiosis. We hypothesize that a potential change in nutrient stoichiometry in the ETNA
22 might lead to a general shift within the diazotrophic community, potentially influencing primary
23 productivity and carbon export.

24 **1 Introduction**

25 Eastern boundary upwelling systems are characterized by cold, nutrient-rich water masses that are
26 transported from intermediate water layers towards the surface. The resulting extensive primary
27 production forms the basis for high biomass development and a productive food web (Pennington et
28 al., 2006). At the same time, biological degradation at depth and weak interior ventilation cause
29 permanently low oxygen concentrations in intermediate water masses (100 – 900 m, Karstensen et
30 al., 2008). These low oxygen conditions support denitrification and anammox that remove bioavailable
31 nitrogen (N) from the water column (e.g. Codispoti et al., 2001; Lam et al., 2009; Kalvelage et al.,
32 2011). Oxygen minimum zones (OMZs) also influence the availability of inorganic phosphate (P),
33 silicon (Si) and trace elements such as iron (Fe), which are released at the sediment-water interface
34 under oxygen deficient conditions (Ingall and Jahnke, 1994; Hensen et al., 2006). Subsequently, the
35 elemental stoichiometry of inorganic nutrients (N:P) in upwelled water masses is below the Redfield
36 ratio of 16:1 (Redfield, 1958), which manifests itself as an excess of P (P^*) relative to N ($P^* = PO_4^{3-} -$
37 $NO_3^-/16$, after Deutsch et al. (2007).

38 In the Eastern Tropical North Atlantic (ETNA) nutrient concentrations and stoichiometry within the
39 euphotic layer cover a wide range. Water masses in coastal regions feature low N:P ratios mainly as a
40 result of benthic N-loss along with P leaching from the sediment (Trimmer and Nicholls, 2009;
41 Jaeschke et al., 2010; Schafstall et al., 2010) suggesting an N limitation of primary production in OMZ-
42 influenced surface waters (Deutsch et al. 2007). In the transition zone between coastal upwelling and
43 open ocean, N:P ratios approach Redfield proportions (Moore et al., 2008). Nevertheless, the
44 nitracline tends to be deeper than the phosphocline in the ETNA (Hausse et al., 2013; Sandel et al.,
45 2015), which also points towards a deficiency of N over P in the euphotic zone. In the Central and
46 West Atlantic, N:P ratios beyond 30:1 can be reached (Fanning, 1992; Moore et al., 2008), suggesting
47 a severe P limitation of primary producers (Ammerman et al., 2003; Mills et al., 2004). Additional input
48 of atmospheric anthropogenic nitrogen into the open ocean could further increase this P deficit in the
49 future (Duce et al., 2008). Oxygen concentrations within the oxygen minimum in the ETNA are usually
50 above $40 \mu\text{mol kg}^{-1}$ and thus considered too high to support N loss processes in the water column
51 (Karstensen et al., 2008; Löscher et al., 2012; Ryabenko et al., 2012). However, recent observations
52 of very low oxygen levels just below the mixed layer associated to anticyclonic modewater eddies
53 suggest a potential for localized denitrification – with an accompanied decrease in N:P ratios – in the
54 open ocean of the ETNA (Karstensen et al., 2015).

55 Discrepancies from the canonical N:P ratio are known to influence productivity and composition of
56 primary producers (Grover, 1997). Since the average elemental composition of N and P in seawater
57 as well as in phytoplankton is 16:1, a deviation of dissolved inorganic nutrients from this ratio could
58 indicate which nutrient can potentially become limiting before the other (Lagus, 2004; Moore et al.,
59 2013). Transferring this concept to upwelling regions with inorganic N:P ratios below Redfield, one
60 would expect that the limiting nutrient for phytoplankton growth in those areas is N. It has been shown,
61 however, that certain functional ecotypes of phytoplankton differ in their required nutrient ratio, as
62 specific cellular entities (e.g. chlorophyll, proteins or rRNA) of primary producers have a unique
63 stoichiometric composition deviating from the classical Redfield stoichiometry (Geider and La Roche,
64 2002; Quigg et al., 2003; Arrigo, 2005). Thus, surface waters adjacent to OMZs potentially provide a

65 niche for certain types of primary producers, whose growth strategy and metabolic requirements are
66 favored by low ratios of N:P. Arrigo (2005) refers to them as „bloomers“ and characterizes them as
67 organisms adapted to exponential growth, which contain high amounts of ribosomes and P-rich rRNA.
68 Those organisms build their biomass in non-Redfield-proportions and exhibit low cellular N:P ratios.
69 The deficit in inorganic N of water masses adjacent to OMZs would thus be reduced by this non-
70 Redfield production and N:P ratios further offshore would approach Redfield conditions.

71 Another concept of phytoplankton growth in N deficient waters is that inorganic nutrients are taken up
72 in Redfield proportion by primary producers, which leaves the surface water masses enriched in P.
73 Excess phosphate presence has been hypothesized to favor N₂-fixation (Deutsch et al., 2007). The
74 conversion of readily available dissolved N₂ into bioavailable forms of fixed N by diazotrophs could
75 replenish the N-deficit in surface waters adjacent to OMZs.

76 Previous bioassay studies that were conducted to identify controlling factors for primary production in
77 the eastern Atlantic using inorganic N, P and dissolved Fe addition, determined N as the key limiting
78 nutrient (e.g. (Graziano et al., 1996; Mills et al., 2004; Moore et al., 2008). These findings are in
79 accordance with an on-board mesocosm study from the same area, where phytoplankton growth
80 depended on the initial supply of N rather than on the N:P ratio and where a combined addition of N
81 and P did not further increase biomass production compared to the addition of N sources alone (Franz
82 et al., 2012). Additionally, the authors deduced that at low N:P ratios excess P was assimilated by
83 non-diazotrophic phytoplankton and was channeled into dissolved organic phosphorus (DOP). As
84 DOP might serve as an additional source of P for bacteria and phytoplankton (Mahaffey et al., 2014
85 and references therein) and is preferentially taken up by the filamentous diazotrophic cyanobacterium
86 *Trichodesmium* (Dyhrman et al., 2006; Sohm and Capone, 2006), it has been proposed that N₂
87 fixation might be stimulated by an enhanced DOP supply under low N:P ratios (Franz et al., 2012).

88 Until recently, oceanic N₂ fixation was mainly attributed to phototrophic cyanobacteria, such as
89 *Trichodesmium* or *Crocospaera*, which are restricted to nutrient depleted surface to subsurface
90 waters due to their light demand (Capone et al., 1997; Zehr and Turner, 2001). However, several
91 groups of non-cyanobacterial diazotrophs and cyanobacterial symbionts have been detected in
92 various oceanic regions, thus demonstrating the ubiquity and high diversity of diazotrophs (Foster et
93 al., 2009; Farnelid et al., 2011; Loescher et al., 2014). Despite the growing awareness of diazotrophic
94 diversity and distribution, the environmental conditions controlling diazotrophy are still not well
95 understood. However temperature, Fe and P availability and dissolved oxygen concentrations are
96 regarded as key factors for diazotrophic distribution and partly for active N₂ fixation (e.g. Sohm et al.,
97 2011). The presence of high amounts of fixed N is thought to inhibit N₂ fixation (Weber and Deutsch,
98 2014), since diazotrophs are either outcompeted by fast growing phytoplankton species such as
99 diatoms (Bonnet et al., 2009; Monteiro et al., 2011), or they themselves take up bioavailable forms of
100 N rather than use the energy consuming process of N₂ fixation (Mulholland and Capone, 2001;
101 Mulholland et al., 2001; Dekaezemacker and Bonnet, 2011).

102 In the ETNA, upwelling of N depleted waters along with high Fe input via Saharan dust deposition
103 (Gao et al., 2001) sets a classical niche for N₂ fixation, while high N:P ratios beyond the upwelling
104 region of the ETNA point towards P limitation of diazotrophs (Ammerman et al., 2003; Mills et al.,
105 2004). Nevertheless, a diverse community of cyanobacterial diazotrophs such as *Trichodesmium*

106 (Capone et al., 1997; Tyrrell et al., 2003), a variety of unicellular cyanobacterial diazotrophs (Groups A,
107 B, C, diatom-symbionts) (Falcon et al., 2002; Langlois et al., 2005) as well as non-cyanobacterial
108 diazotrophs such as different clades of proteobacteria are abundant and widely distributed (e.g.
109 (Langlois et al., 2005; 2008). Those diazotrophs have previously been demonstrated to actively fix N₂
110 in the ETNA (Langlois et al., 2005; 2008; Foster et al., 2009), showing highest rates in nutrient
111 depleted surface to subsurface waters (Großkopf et al., 2012).

112 We investigated the effect of variable nitrate and phosphate supply on phytoplankton growth and
113 addressed the diazotrophic response to changes in N:P stoichiometry over time in two consecutive
114 mesocosm experiments. In order to extend the design of previous mesocosm experiments (Franz et
115 al., 2012), N and P supply ratios were varied while keeping either nitrate or phosphate at constant
116 concentrations. High N:P ratios were applied to investigate potential inhibition of N₂ fixation, while low
117 N:P supply ratios were applied to unravel the role of excess P and consecutively formed DOP on
118 primary production and diazotrophy. Direct N₂ fixation rate measurements as well as determination of
119 *nifH* gene and transcript abundances were carried out to characterize the diazotrophic community and
120 their response to the chosen treatment levels. The experimental design and response variables were
121 chosen in order to assess responses of the phytoplankton community to possible changes in oceanic
122 nutrient stoichiometry as a consequence of ocean deoxygenation.

123

124 2 Methods

125 2.1 Experimental Setup

126 In October 2012 we conducted two 8-day mesocosm experiments at the Instituto Nacional de
127 Desenvolvimento das Pescas (INDP), Mindelo, Cape Verde. The night before the start of each
128 experiment, surface water was collected with RV *Islândia* south of São Vicente (16°44.4'N, 25°09.4'W)
129 and transported to shore using four 600 L food safe intermediate bulk containers. Containers for water
130 transport were first rinsed with diluted HCl and several times with deionized water. The experimental
131 setup comprised sixteen plastic mesocosm bags, which were distributed in four flow-through water
132 baths. Blue, transparent lids were added to reduce the light intensity to approximately 20 % of surface
133 irradiation. The collected water was evenly distributed among mesocosm bags by gravity, using a
134 submerged hose to minimize bubbles. The volume inside each mesocosm was calculated after adding
135 1.5 mmol silicic acid and measuring the resulting silicic acid concentration. The volume ranged from
136 105.5–145 liters. Nutrients in all mesocosms were measured before nutrient manipulation. Nitrate
137 (NO_3^-), nitrite (NO_2^-), phosphate (PO_4^{3-}) and silicic acid ($\text{Si}(\text{OH})_4$) were all below the detection limit and
138 far below the manipulation levels (see Fig. 2). We therefore conclude that no contamination with these
139 nutrients occurred during water sampling, transport and mesocosm filling. Experimental manipulation
140 was achieved by adding different amounts of nitrate and phosphate. In the first experiment, the
141 phosphate supply was changed at constant nitrate supply (*varied P*) in thirteen of the sixteen units,
142 while in the second experiment the nitrate supply was changed at constant phosphate supply (*varied*
143 *N*) in twelve of the sixteen units. Each of these nutrient treatments was replicated 3 times. In addition
144 to this, „cornerpoints“ were chosen, where both the nitrate and phosphate supply was changed. The
145 „cornerpoints“ were not replicated. These treatments were repeated during both experiments (see Fig.
146 1 for experimental design). Four cornerpoints should have been repeated, but due to erroneous
147 nutrient levels in mesocosm 10 during *varied N*, this mesocosm also was adjusted to the center point
148 conditions. Experimental treatments were randomly distributed between the four water baths. Initial
149 sampling was carried out immediately after filling of the mesocosms on day 1. After nutrient
150 manipulation, sampling was conducted on a daily basis between 09:00 and 10:30 for days 2 to 8.
151 Nutrient levels were set between 2 and 20 $\mu\text{mol L}^{-1}$ for nitrate, 0.25 and 1.75 $\mu\text{mol L}^{-1}$ for phosphate
152 and 15 $\mu\text{mol L}^{-1}$ for silicic acid. Table S1 gives the target nutrient concentrations and corresponding
153 measured concentrations in the mesocosms.

154 It has to be noted, that no algal bloom developed in mesocosm 5 during *varied N* (target
155 concentrations: 17.65 $\mu\text{mol L}^{-1}$ NO_3^- , 0.40 $\mu\text{mol L}^{-1}$ PO_4^{3-}). Thus, it was not included in the analysis and
156 data are not presented.

157 Although we refer to our experimental approach as mesocosm experiment, this label might be
158 disputable depending on the definition of the term mesocosm. Sometimes, experimental enclosures
159 are only defined by size, where our approach would fall into the range of a microcosm experiment
160 ($<1 \text{ m}^3$; Riebesell et al., 2010). Independent of its size, a mesocosm can also be defined as a confined
161 body of water, where environmental factors are manipulated at the community or ecosystem level
162 (Stewart et al., 2013). In contrast, microcosm experiments are often used to manipulate factors at the
163 population level and often lack the realism to extrapolate results to natural systems (Stewart et al.,
164 2013). Although our experimental enclosures are limited in size, we consider it justified using the term

165 mesocosm, as we conducted our experiments with natural communities consisting of at least 3 trophic
166 levels (bacteria, phytoplankton, microzooplankton).

167

168 **2.3 Nutrients**

169 Samples (10 mL) for dissolved inorganic nutrients (NO_3^- , NO_2^- , PO_4^{3-} , $\text{Si}(\text{OH})_4$) were taken daily from
170 each mesocosm and measured directly using a QuAatro Autoanalyzer (Seal Analytic) according to
171 Grasshoff et al. (1999). The detection limits of nutrient analyses were $0.01 \mu\text{mol L}^{-1}$ for NO_2^- and PO_4^{3-} ,
172 $0.03 \mu\text{mol L}^{-1}$ for NO_3^- and $0.04 \mu\text{mol L}^{-1}$ for $\text{Si}(\text{OH})_4$.

173

174 **2.4 Chlorophyll a**

175 For chlorophyll a (Chl a) analyses, water samples (0.5 – 1 L) were vacuum-filtered (200 mbar) onto
176 Whatman GF/F filters (25 mm, $0.7 \mu\text{m}$) before adding 1 ml of ultrapure water. Filters were immediately
177 stored frozen for at least 24 hours. 9 ml acetone (100 %) was then added to each sample and the
178 fluorescence was measured with a Turner Trilogy fluorometer, which was calibrated with a Chl a
179 standard dilution series (*Anacystis nidulans*, Walter CMP, Kiel, Germany). Chl a concentrations were
180 determined according to Parsons et al. (1984).

181

182 **2.5 Dissolved organic phosphorus**

183 Water samples for analyses were filtered through pre-combusted (450°C , 5 hours) Whatman GF/F
184 filters (25 mm, $0.7 \mu\text{m}$). The filtrate was stored in acid-clean 60 ml HDPE bottles (5 % HCl for at least
185 12 hours) and frozen at -20°C until further analysis.

186 Prior to analysis of total dissolved phosphorus (TDP) one metering spoon of the oxidizing reagent
187 Oxisolv (Merck) was added to 40 ml of sample, which was hereupon autoclaved for 30 minutes.
188 Samples were then analysed spectrophotometrically (Autoanalyzer QuAatro Seal Analytic), following
189 Bran and Luebbe AutoAnalyzer Method No. G-175-96 Rev. 13 (PO_4^{3-}). The detection limit was
190 $0.2 \mu\text{mol L}^{-1}$ and analytical precision was $\pm 8.3\%$.

191 DOP concentrations were calculated as:

192

$$193 \text{DOP} = \text{total dissolved phosphorus (TDP)} - \text{dissolved inorganic phosphate (PO}_4^{3-}) \quad (1)$$

194

195 **2.6 Particulate organic matter**

196 Particulate organic matter concentrations were determined by filtering 0.5 – 1 L seawater through pre-
197 combusted (450°C for 5 hours) Whatman GF/F filters (25 mm, $0.7 \mu\text{m}$) under low pressure (200 mbar).
198 Filters were immediately frozen and stored until analysis.

199 Prior to analysis, particulate organic carbon (POC) and nitrogen (PON) filters were fumed with HCl
200 (37 %, for 24 hours) in order to remove inorganic carbon. After drying, filters were wrapped in tin cups
201 ($8 \times 8 \times 15 \text{ mm}$) and measured according to Sharp (1974) using an elemental analyzer (Euro EA,
202 EuroVector, Milan, Italy).

203 For particulate organic phosphorus (POP) measurements, filters were autoclaved with the oxidation
204 reagent Oxisolv (Merck) and 40 ml of ultrapure water for 30 min in a pressure cooker. Then,
205 orthophosphate was analyzed photometrically according to Hansen and Koroleff (1999).

206

207 Relationships of dissolved and particulate organic matter accumulation to the inorganic nutrient supply
208 ratios were determined using Model I regression analyses (SigmaPlot, Systat).

209

210 **2.7 Molecular methods**

211 Samples for the extraction of DNA/RNA were taken by filtering a volume of 1–2 L (exact volumes and
212 filtration times were determined and recorded continuously) of seawater through 0.2 μm
213 polyethersulfon membrane filters (Millipore, Billerica, MA, USA). The filters were frozen and stored at -
214 80 °C until analysis. Nucleic acid extraction was performed using the Qiagen DNA/RNA All prep Kit
215 (Qiagen, Hilden, Germany) according to the manufacturer's protocol. The extracted RNA was reverse
216 transcribed to cDNA using the Superscript III First Strand synthesis Kit (Invitrogen) following the
217 manufacturer's protocol with primers *nifH2* and *nifH3* (Langlois et al., 2005; Zani et al., 2000). *NifH*
218 clusters were quantified from DNA and cDNA by quantitative Real Time PCRs as previously described
219 by Church et al. (2005) and Langlois et al. (2008). TaqMan® qPCRs were set up in 12.5 μl reactions
220 and were performed in technical duplicates in an ABI ViiA7 qPCR system (Life technologies, Carlsbad,
221 CA, USA). For each primer and probe set, standard curves were obtained from dilution series ranging
222 from 10^7 to 10 gene copies per reaction; standards were constructed using plasmids containing the
223 target *nifH* gene. Sequences of primers and probes are given in Table 1. To confirm purity of RNA,
224 non-template qPCRs were performed using the corresponding RNA.

225

226 **2.8 $^{15}\text{N}_2$ seawater incubations**

227 Seawater incubations were performed in triplicates from each mesocosm on day 1 and day 8 of both
228 experiments as previously described by Mohr et al. (2010) and Großkopf et al. (2012). Degassed
229 seawater was filled into evacuated gas-tight 3L Tedlar® bags without a headspace. Addition of $^{15}\text{N}_2$
230 gas was (depending on the exact water volume in the Tedlar® bag) around 10 ml $^{15}\text{N}_2$ per 1 L
231 seawater. Dissolution of the $^{15}\text{N}_2$ gas was achieved by 'slapping' the bubble with a ruler. After
232 complete dissolution of the added $^{15}\text{N}_2$ gas ($^{15}\text{N}_2$ -enriched seawater), an aliquot of the $^{15}\text{N}_2$ enriched
233 water was collected for each preparation of enriched seawater and stored in an Exetainer. Seawater
234 samples were filled headspace-free; 100 ml of seawater were exchanged with previously degassed
235 seawater containing a defined concentration $^{15}\text{N}_2$ and ^{13}C -NaCO. Incubations were performed in 4.5 L
236 polycarbonate bottles closed with Teflon®-coated butyl rubber septum caps. The $^{15}\text{N}_2$ concentration in
237 the prepared batches of enriched water was determined to be 250 $\mu\text{mol L}^{-1}$, which translates in an ^{15}N -
238 enrichment of about 2 % in the 4.5 L bottle incubations, when adding 100 mL enriched seawater
239 (depending on temperature and salinity). Water samples were incubated for 24 hours in the
240 mesocosm water baths, thus at the same temperature and light regime, followed by a filtration on
241 Whatman GF/F filters, which were analyzed using mass spectrometry as previously described in
242 Loescher et al. (2014).

243

244 **3. Results**

245 **3.1 Bloom development and nutrient dynamics in the mesocosms**

246 In both consecutive experiments (*varied P* and *N*) a bloom formation was observed following nutrient
247 manipulation. Nitrate and phosphate were readily taken up by the plankton community and nutrient
248 concentrations thus declined until the end of the experiment (Fig. 2). NO_3^- was fully depleted in all
249 mesocosms at days 6–8 in both runs, except in the mesocosms with highest N:P ratios of 48:1
250 (treatment 12.00N/0.25P in *varied P*) and 44:1 (treatment 17.65N/0.40P in *varied N*). Residual PO_4^{3-}
251 was still detectable at the end of the experiments (day 8) in all mesocosms with initial N:P values <10
252 (treatments in *varied P*: 6.35N/1.10P, 12.00N/1.25P, 12.00N/1.75P; treatments in *varied N*:
253 2.00N/0.75P, 4.00N/0.75P, 6.00N/1.03P) indicating a limitation of primary productivity dependent on
254 the N:P ratio.

255 Although initial Chl *a* concentrations were slightly higher in *varied P* than in *varied N* ($\sim 0.38 \mu\text{g L}^{-1}$ and
256 $0.2 \mu\text{g L}^{-1}$, respectively), the increase in Chl *a* concentration was 5–10-fold until days 5/6 in *varied P*
257 compared to 10–50-fold in *varied N*. After the bloom at days 5 and 6 Chl *a* declined again to 0.05–
258 $0.7 \mu\text{g L}^{-1}$ and $0.6\text{--}1.7 \mu\text{g L}^{-1}$ in *varied P* and *varied N*, respectively (Fig. 2).

259

260 **3.2 Particulate organic matter (POM) accumulation and stoichiometry**

261 Temporal dynamics of POM were similar during both experiments. Initial concentrations of POC, PON
262 and POP were $10\text{--}17 \mu\text{mol L}^{-1}$, $1.5\text{--}2 \mu\text{mol L}^{-1}$ and $0.05\text{--}0.12 \mu\text{mol L}^{-1}$, respectively (Fig. 2). In *varied*
263 *P*, POC and PON reached a maximum on day 6, while POP increased until the end of the experiment.
264 In *varied N* POM accumulation also peaked on day 6 or 7 in most mesocosms, but differences
265 between N:P treatments were more pronounced in *varied N* compared to *varied P*. Our results indicate
266 that POM accumulation was independent of the initial nutrient supply ratio in both experiments (Fig. 3).
267 We observed a significantly positive regression coefficient between maximum POC and PON
268 concentrations (defined as peak POC and PON concentration subtracted by the initial (day 1) POC
269 and PON concentration) to the initial NO_3^- supply (POC: $r^2 = 0.64$, $p = 0.0006$; PON: $r^2 = 0.80$, $p <$
270 0.0001) while POP accumulation showed a significantly positive regression coefficient to initial PO_4^{3-}
271 supply ($r^2 = 0.31$, $p = 0.048$).

272 Mean PON:POP ratios during the exponential growth phase appeared to be independent of the initial
273 N:P supply ratio in both experimental runs (Fig. 4). With ratios between 17 and 23, the PON:POP
274 ratios were above, but close to Redfield proportion in all treatments during the first 5 days of the
275 experiments, consistent with an observed initial uptake of N:P in Redfield proportions in all
276 mesocosms. During the post bloom phase, mean PON:POP ratios were positively correlated with the
277 initial nutrient supply ratio ($r^2 = 0.73$, $p < 0.0001$). Nevertheless, stoichiometry of POM (N:P between
278 16 and 32) exceeded Redfield proportions, even in treatments with lowest N:P ratios.

279

280 **3.3 Dissolved organic phosphorus dynamics**

281 Initial DOP concentrations during *varied P* were $0.14 (\pm 0.009) \mu\text{mol L}^{-1}$. In most mesocosms, except
282 for the one with lowest initial PO_4^{3-} supply (12.00N/0.25P), DOP concentrations increased
283 progressively until the end of the experiment (Fig. 5). Highest DOP concentrations of around
284 $0.4 \mu\text{mol L}^{-1}$ were determined in mesocosm 12.00N/0.75P on day 5 and decreased again afterwards.
285 Maximum DOP accumulation (defined as described for maximum POM accumulation, section 3.2)
286 was significantly correlated to the initial PO_4^{3-} supply (Fig. 5; $r^2 = 0.63$, $p = 0.0007$).

287 In *varied N* initial DOP concentrations in the mesocosms were $0.2 (\pm 0.038) \mu\text{mol L}^{-1}$ and increased
288 slightly until day 3. Afterwards DOP concentrations remained rather constant, although with
289 considerable variability in the data (Fig. 5).

290 A simple mass balance (Table S2) showed that part of the phosphorus pool, i.e. the sum of PO_4^{3-} ,
291 DOP and POP, remained unaccounted for (P pool_x) at the end of the experiment (P pool_x in *varied P*
292 ~25% of the initial P pool, P pool_x in *varied N* ~14%). This undetermined P pool is most likely due to
293 wall growth, which became visible towards the end of the experiment. However, only in two
294 mesocosms the difference between P pools sizes on day 2 and day 8 was significant.

295

296 **3.4 Importance of the *Richelia-Rhizosolenia* symbiosis for diazotrophy**

297 Directly measured rates of N_2 fixation showed an increase with time in *varied P*, while no statistically
298 significant increase could be observed in *varied N* (Fig. 6).

299 A molecular screening of the diazotrophic community in the initial water batch used for *varied P* using
300 the *nifH* gene as functional marker gene showed a dominance of filamentous cyanobacterial
301 diazotrophs related to *Trichodesmium* accounting for ~54% of the diazotrophic community (results
302 from qPCR), followed by proteobacterial diazotrophs (~36%) in *varied P* (data not shown). The high
303 abundance of filamentous cyanobacterial diazotrophs indicated the presence of a bloom in the initial
304 water batch in *varied P*. In *varied N*, the initial community consisted mainly of proteobacterial
305 diazotrophs (~88%), followed by UCYN-B (9%) and filamentous cyanobacteria (3%).

306 Changes in transcript abundance over time were most intense for *Richelia-Rhizosolenia* (Het I)
307 transcripts (Fig. 8). At day 2, Het I transcript abundances were higher in *varied N* conditions compared
308 to *varied P*. This relation changed over the course of the experiments, with a pronounced increase of
309 Het I transcript abundances between day 6 and 8 in *varied P*.

310 Thus, all classical *nifH* clusters (filamentous cyanobacteria, UCYN-A, -B, -C and proteobacteria
311 diazotrophs) decreased in abundance of genes and gene transcripts down to the detection limit in both
312 experiments, whereas diazotrophs of the *Richelia-Rhizosolenia* symbiosis were the only diazotrophs
313 that showed an increase in *nifH* transcripts over the course of the experiment, exclusively in *varied P*
314 (Fig. 8). During *varied N*, *nifH* gene and transcript abundance of the *Richelia-Rhizosolenia* cluster was
315 close to the detection limit and DOP accumulation was rather negligible. In contrast, we observed an
316 accumulation of DOP in *varied P*. Here, mesocosms with a significant increase in N_2 fixation
317 (12.00N/0.25P and 12.00/0.75P) were also the ones where DOP was used as phosphorus-source for
318 biomass build up after PO_4^{3-} was depleted (Fig. 9). In mesocosm 12.00N/0.75P, PO_4^{3-} concentrations
319 were below the detection limit after day 5. This coincided with a decrease of DOP after day 5, while
320 POP concentrations increased until the end of the experiment. In mesocosm 12.00N/0.25P, POP also
321 increased beyond the point of PO_4^{3-} depletion and highest POP accumulation exceeded values that
322 could be explained by PO_4^{3-} incorporation alone. Thus a potential impact of DOP on diazotrophy is
323 hypothesized. In mesocosms without a significant increase in N_2 fixation, POP and DOP
324 concentrations increased until the end of the experiment and no apparent uptake of DOP could be
325 observed.

326

327 **4 Discussion**

328 **4.1 Controls on plankton production**

329 In order to understand potential consequences of changes in nutrient regimes, it is necessary to
330 determine the factors that control and limit microbial production. In our experiments, amendments of
331 NO_3^- significantly increased chlorophyll concentrations and enhanced the accumulation of POM,
332 indicating the ability of the plankton community to rapidly and intensively react to nitrate availability.
333 These results suggest that the ultimate limiting nutrient for phytoplankton production in our experiment
334 was NO_3^- . N_2 fixation was measurable in all initial samples, which indicates the presence of a niche for
335 diazotrophs in the Cape Verde region. For the upwelling region as well as for the oligotrophic open
336 ocean of the ETNA, nitrate limitation of the phytoplankton community has previously been reported
337 (Davey et al., 2008; Moore et al., 2008; Franz et al., 2012). Additionally, Moore et al. (2008) observed
338 a co-limitation of nitrate and phosphate during nutrient addition bioassay experiments in the ETNA. In
339 our experiment, however, only POP accumulation was positively affected by PO_4^{3-} supply. This argues
340 against a secondary limitation by phosphate, but rather points towards a mechanism of accumulating
341 and storing phosphate as polyphosphate within the cell (Schelske and Sicko-Goad, 1990; Geider and
342 La Roche, 2002; Martin et al., 2014).

343 There is a large difference between the supply ratio of inorganic nutrients and the PON:POP ratio of
344 the plankton community in our study. Although initial N:P ratios in our mesocosms covered a wide
345 range, PON:POP ratios reached maximum values of ~21 in both experiments during the exponential
346 growth phase. During stationary growth, maximum PON:POP values of 39 in *varied N* and 22 in *varied P*
347 were measured. However, during growth phases in both experiments PON:POP ratios did never fall
348 below 16. Very similar results were obtained by Franz et al (2012) off the Peruvian coast. However,
349 two experiments conducted by Franz et al. (2012) in the ETNA and off West Africa showed a different
350 response of the phytoplankton community. In these two cases, N:P supply ratio and PON:POP were
351 highly correlated and PON:POP ratios as low as 6.0 (± 1.4) were observed in the stagnant phase. This
352 shows that the stoichiometry of phytoplankton communities is flexible to a certain extent, but does not
353 necessarily reach dimensions observed in laboratory experiments (Hecky et al., 1993) and implied by
354 theoretical approaches (e.g. Geider and La Roche, 2002; Klausmeier et al., 2004). This may result
355 from differences in the initial community composition if it lacks organisms able to assemble a P-rich
356 growth machinery (Klausmeier et al., 2004; Arrigo, 2005). It has been reported that cellular N content
357 seems relatively inflexible in some phytoplankton groups, thus restricting the maintenance of
358 metabolic processes at low dissolved inorganic nitrogen concentrations (Moore et al., 2013). In
359 contrast, phosphate requirements seem to be comparably flexible, as certain cellular components
360 containing P (e.g. phospholipids) can be replaced by non-phosphorus containing compounds (Moore
361 et al., 2013). This can also be deduced from our experiments, where higher N:P ratios lead to
362 increasing PON:POP ratios, possibly due to the flexibility to substitute P compounds within the
363 biomass. In contrast, lower N:P ratios lead to lower biomass accumulation, as the plasticity of
364 PON:POP seems to be constrained by the availability of nitrate in our experiments.

365

366 **4.2 The impact of bioavailable N on N_2 fixation**

367 The ability of diazotrophs to grow independent of a fixed N source in principle gives them an
368 advantage to thrive under conditions where their competitors are limited by N availability. At the same
369 time, diazotrophs are considered disadvantaged when competing with faster growing non-diazotrophs
370 for nutrients under N replete conditions (Tyrrell, 1999; Ward et al., 2013). Contrary to this classical
371 view, we could not detect a direct influence of reactive N compounds on N₂ fixation in our experiments.
372 Despite a wide spectrum of applied nitrate concentrations in *varied N*, no significant difference in N₂
373 fixation rates could be detected. Evidence from culture experiments also suggests that inorganic N
374 compounds do not always repress N₂ fixation. While NO₃⁻ addition in *Trichodesmium* spp. (Mulholland
375 et al., 2001; Holl and Montoya, 2005) and NH₄⁺ addition in *Crocospaera watsonii* (Dekaezemaker
376 and Bonnet, 2011) reduced N₂ fixation rates, NO₃⁻ addition did not reduce N₂ fixation rates in *C.*
377 *watsonii* and *Nodularia* spp. cultures (Sanz-Alferez and del Campo, 1994; Dekaezemaker and
378 Bonnet, 2011). Moreover, recent field surveys demonstrated the occurrence of N₂ fixation in nutrient
379 rich water masses of the eastern tropical South Pacific (ETSP) and equatorial Atlantic upwelling
380 regions (Fernandez et al., 2011; Subramaniam et al., 2013; Loescher et al., 2014) and also modelling
381 studies predict high N₂ fixation rates in waters containing measurable amounts of reactive N (Deutsch
382 et al., 2012; Weber and Deutsch, 2014). Clearly, the degree of feedback concerning the inhibition of
383 N₂ fixation by reactive N compounds is not universal and there is evidence that the absence of P and
384 Fe in seawater is a stronger indicator for limitation of N₂ fixation than the presence of inorganic N
385 compounds (Weber and Deutsch, 2014).

386

387 **4.3 The role of excess P and DOP as controls on N₂ fixation**

388 Deutsch et al. (2007) suggested that N₂ fixation is favored in upwelling regions, where N loss in
389 adjacent OMZ waters and P leaching from the sediment lead to upwelling of waters enriched in P. This
390 excess P is thought to be consumed by diazotrophs, thus replenishing the N-deficit in the vicinity of
391 upwelling regions.

392 As nutrients were taken up in Redfield or above Redfield proportions in our experiments we would
393 have expected excess phosphate in mesocosms with N:P supply ratios below Redfield. Instead,
394 excess phosphate was absent and our data point towards a channeling of PO₄³⁻ through the
395 particulate pool into DOP, as an increase in PO₄³⁻ supply significantly increased the concentration of
396 DOP. Why phytoplankton synthesize and excrete higher levels of DOP under excess phosphate
397 conditions remains unclear, but enhanced PO₄³⁻ uptake (followed by DOP accumulation) is thought to
398 hamper P limitation when sudden boosts in N are encountered (Mackey, 2012). In accordance with
399 our study, mesocosm experiments from the ETNA and eastern tropical south Pacific (ETSP) open
400 ocean (Franz et al., 2012) and measurements from shelf regions of the ETNA (Reynolds et al., 2014)
401 and Celtic Sea (Davis et al., 2014) showed the accumulation of DOP under excess phosphate supply.
402 Although the composition and bioavailability of the DOP pool needs to be further evaluated, DOP may
403 act as a source of P for prokaryotic primary producers, either exclusively or in addition to PO₄³⁻
404 (Björkman and Karl, 2003; Dyrman et al., 2006; Mahaffey et al., 2014; Reynolds et al., 2014). This
405 indicates that the ability to utilize DOP may give diazotrophs a competitive advantage when
406 bioavailable forms of N are depleted and either PO₄³⁻ or DOP concentrations are sufficient.

407 In our experiments a significant increase in N₂ fixation rates was only detected in *varied P*. In
408 mesocosms with highest N₂ fixation rates, PO₄³⁻ was depleted after day 5 or 6 while POP increased
409 until the end of the experiment. After PO₄³⁻ depletion, DOP concentrations declined, which indicates
410 that DOP served as phosphorus source until the end of the experiment. It has to be noted that N₂
411 fixation rates were only measured at the beginning and the end of our experiment and possible
412 fluctuations over time cannot be accounted for. However, increasing diazotrophic transcript
413 abundances of *Richelia intracellularis* in symbiosis with the diatom *Rhizosolenia* (Het I) were also
414 detected over the course of the *variable P* experiment. While the diatom abundance was probably
415 favored by replete amounts of silicic acid added at the beginning of the experiment, no increase in
416 diatom-diazotroph associations (DDAs) was detected in the *varied N* experiment. Measured N₂ fixation
417 rates and transcript abundances lead us to speculate that DDAs were favored in the *varied P*
418 experiment, where diazotrophs in the mesocosms utilized DOP resources in order to supply P to
419 themselves and/or their symbiont. The ability to utilize DOP has previously been shown for *R.*
420 *intracellularis* (Girault et al., 2013) and our observations suggest that they may not only provide their
421 symbionts with N via N₂ fixation but also with P via DOP utilization.

422 DDAs in our experiment were favored by replete amounts of silicic acid and DOP and were – in
423 contrast to the classical view – not restrained by reactive N compounds. These findings suggest that
424 DDAs have the potential to actively fix nitrogen in shelf waters of upwelling regions. Therefore, the N-
425 deficit of upwelled water-masses could already be replenished locally prior to offshore transport.

426 A shift within the diazotrophic community towards DDAs could also exert controls on carbon export.
427 Grazing, particle aggregation and export likely increase when filamentous and proteobacterial
428 cyanobacteria are replaced by DDAs (e.g. Karl et al., 2008; 2012). The enhanced strength and
429 efficiency of the biological pump would therefore increase the potential for carbon sequestration in the
430 ETNA.

431

432 **5 Conclusions and future implications for ETNA**

433 Our findings add to the growing evidence that diminished N:P ratios in upwelling waters in the ETNA
434 will either decrease the biomass of non-diazotrophic primary producers, specifically due to the decline
435 of bioavailable N, or lead to a community shift towards primary producers that are able to adapt to
436 changing N:P conditions. As a considerable amount of DOP was produced under excess phosphate
437 conditions, changes in the N:P ratio of waters could exert profound control over DOP production rates
438 in the ETNA. Our results indicate that enhanced DOP production in upwelling regions will likely fuel N₂
439 fixation, with an advantage for those diazotrophs capable of DOP utilization. We propose that N₂
440 fixation in the ETNA might not only be restricted to the oligotrophic open ocean but can occur in
441 nutrient-rich upwelling regions as previously demonstrated for the tropical Pacific (Löscher et al.,
442 2014) and the Atlantic equatorial upwelling (Subramanian et al., 2013), as N₂ fixation in DDAs seems
443 to be favored by the presence of silicic acid and DOP, and not by the absence of fixed N compounds.

444

445

446 **Acknowledgements**

447 The authors thank their colleagues from the INDP, Cape Verde for their assistance with setting up the
448 experiment. We further acknowledge the captain and crew of RV Islandia. We thank Ulrike Panknin,
449 João Gladek, Ivanice Monteiro, Nuno Viera, Elizandro Rodriguez, Miriam Philippi and Chris Hoffmann
450 for technical assistance; further, we thank Alexandra Marki, Jasmin Franz, Harald Schunck and
451 Markus Pahlow for helpful discussion of the results. This study is a contribution of the DFG funded
452 Collaborative Research Center 754 (www.sfb754.de).

453

454 Authors' contribution

455 HH and RK designed the experiment with input from JM, CRL, AL, CB, UR, RAS; led the logistics and
456 the study on site and provided nutrient and hydro-chemical datasets. JM, RK, AFR, AL, CB and HH
457 conducted the sampling of particulate and dissolved matter. JM and AFR performed DOM and POM
458 measurements, CRL performed N₂ fixation and molecular experiments and measurements. JM and
459 CRL wrote the manuscript with input from all co-authors.

460

461 All data will be uploaded at www.pangaea.de upon publication.

462 **References**

- 463 Ammerman, J. W., Hood, R. R., Case, D. A. and Cotner, J. B.: Phosphorus deficiency in the Atlantic:
464 An emerging paradigm in oceanography, *Eos Trans. AGU*, 84(18), 165–170,
465 doi:10.1029/2003EO180001, 2003.
- 466 Arrigo, K. R.: Marine microorganisms and global nutrient cycles, *Nature*, 437(7057), 349–355,
467 doi:10.1038/nature04158, 2005.
- 468 Berthelot, H., Moutin, T., L'Helguen, S., Leblanc, K., Hélias, S., Grosso, O., Leblond, N., Charrière, B.
469 and Bonnet, S.: Dinitrogen fixation and dissolved organic nitrogen fueled primary production and
470 particulate export during the VAHINE mesocosm experiment (New Caledonia lagoon),
471 *Biogeosciences*, 12(13), 4099–4112, doi:10.5194/bg-12-4099-2015, 2015.
- 472 Björkman, K. M. and Karl, D. M.: Bioavailability of dissolved organic phosphorus in the euphotic zone
473 at Station ALOHA, North Pacific Subtropical Gyre, *Limnol. Oceanogr.*, 48(3), 1049–1057,
474 doi:10.4319/lo.2003.48.3.1049, 2003.
- 475 Bonnet, S., Biegala, I. C., Dutrieux, P., Slemmons, L. O. and Capone, D. G.: Nitrogen fixation in the
476 western equatorial Pacific: Rates, diazotrophic cyanobacterial size class distribution, and
477 biogeochemical significance, *Global Biogeochem. Cycles*, 23(3), GB3012,
478 doi:10.1029/2008GB003439, 2009.
- 479 Capone, D. G., Zehr, J. P., Paerl, H. W., Bergman, B. and Carpenter, E. J.: *Trichodesmium*, a globally
480 significant marine cyanobacterium, *Science*, 276(5316), 1221–1229,
481 doi:10.1126/science.276.5316.1221, 1997.
- 482 Church, M. J., Jenkins, B. D., Karl, D. M. and Zehr, J. P.: Vertical distributions of nitrogen-fixing
483 phylotypes at Stn Aloha in the oligotrophic North Pacific Ocean, *Aquat. Microb. Ecol.*, 38(1), 3–14,
484 doi:10.3354/ame038003, 2005.
- 485 Codispoti, L. A., Brandes, J. A., Christensen, J. P., Devol, A. H., Naqvi, S., Paerl, H. W. and Yoshinari,
486 T.: The oceanic fixed nitrogen and nitrous oxide budgets: Moving targets as we enter the
487 anthropocene? *Sci. Mar.*, 65(S2), 85–105, doi:10.3989/scimar.2001.65s285, 2001.
- 488 Davey, M., Tarran, G. A., Mills, M. M., Ridame, C., Geider, R. J. and LaRoche, J.: Nutrient limitation of
489 picophytoplankton photosynthesis and growth in the tropical North Atlantic, *Limnol. Oceanogr.*, 53(5),
490 1722–1733, doi:10.4319/lo.2008.53.5.1722, 2008.
- 491 Davis, C. E., Mahaffey, C., Wolff, G. A. and Sharples, J.: A storm in a shelf sea: Variation in
492 phosphorus distribution and organic matter stoichiometry, *Geophys. Res. Lett.*, 41(23), 8452–8459,
493 doi:10.1002/2014GL061949, 2014.
- 494 De Baar, H.: von Liebig's law of the minimum and plankton ecology (1899–1991), *Progr. Oceanog.*,
495 33(4), 347–386, doi:10.1016/0079-6611(94)90022-1, 1994.
- 496 Dekaezemacker, J. and Bonnet, S.: Sensitivity of N₂ fixation to combined nitrogen forms (NO₃⁻ and
497 NH₄⁺) in two strains of the marine diazotroph *Crocospaera watsonii* (Cyanobacteria), *Mar. Ecol. Prog.
498 Ser.*, 438, 33–46, doi:10.3354/meps09297, 2011.
- 499 Deutsch, C., Sarmiento, J. L., Sigman, D. M., Gruber, N. and Dunne, J. P.: Spatial coupling of nitrogen
500 inputs and losses in the ocean, *Nature*, 445(7124), 163–167, doi:10.1038/nature05392, 2007.
- 501 Deutsch, C., Gruber, N., Key, R. M., Sarmiento, J. L. and Ganachaud, A.: Denitrification and N₂
502 fixation in the Pacific Ocean, *Global Biogeochem. Cycles*, 15(2), 483–506,
503 doi:10.1029/2000GB001291, 2012.
- 504 Deutsch, C., Sarmiento, J. L., Sigman, D. M., Gruber, N. and Dunne, J. P.: Spatial coupling of nitrogen
505 inputs and losses in the ocean, *Nature*, 445(7124), 163–167, doi:10.1038/nature05392, 2007.
- 506 Duce, R. A., LaRoche, J., Altieri, K., Arrigo, K. R., Baker, A. R., Capone, D. G., Cornell, S., Dentener,

- 507 F., Galloway, J., Ganeshram, R. S., Geider, R. J., Jickells, T., Kuypers, M. M., Langlois, R., Liss, P. S.,
508 Liu, S. M., Middelburg, J. J., Moore, C. M., Nickovic, S., Oschlies, A., Pedersen, T., Prospero, J.,
509 Schlitzer, R., Seitzinger, S., Sorensen, L. L., Uematsu, M., Ulloa, O., Voss, M., Ward, B. and Zamora,
510 L.: Impacts of Atmospheric Anthropogenic Nitrogen on the Open Ocean, *Science*, 320(5878), 893–
511 897, doi:10.1126/science.1150369, 2008.
- 512 Dyhrman, S. T., Chappell, P. D., Haley, S. T., Moffett, J. W., Orchard, E. D., Waterbury, J. B. and
513 Webb, E. A.: Phosphonate utilization by the globally important marine diazotroph *Trichodesmium*,
514 *Nature*, 439(7072), 68–71, doi:10.1038/nature04203, 2006.
- 515 Falcon, L. I., Cipriano, F., Chistoserdov, A. Y. and Carpenter, E. J.: Diversity of diazotrophic unicellular
516 cyanobacteria in the tropical North Atlantic Ocean, *Appl. Environ. Microbiol.*, 68(11), 5760–5764,
517 doi:10.1128/AEM.68.11.5760-5764.2002, 2002.
- 518 Fanning, K. A.: Nutrient Provinces in the Sea - Concentration Ratios, Reaction-Rate Ratios, and Ideal
519 Covariation, *J. Geophys. Res.*, 97(C4), 5693–5712, doi:10.1029/92JC00007, 1992.
- 520 Farnelid, H., Andersson, A. F., Bertilsson, S., Abu Al-Soud, W., Hansen, L. H., Sorensen, S., Steward,
521 G. F., Hagstrom, A. and Riemann, L.: Nitrogenase Gene Amplicons from Global Marine Surface
522 Waters Are Dominated by Genes of Non-Cyanobacteria, edited by J. A. Gilbert, *PLoS ONE*, 6(4),
523 doi:10.1371/journal.pone.0019223, 2011.
- 524 Fernandez, C., Farías, L. and Ulloa, O.: Nitrogen Fixation in Denitrified Marine Waters, *PLoS ONE*,
525 6(6), e20539, doi:10.1371/journal.pone.0020539.s007, 2011.
- 526 Foster, R. A., Subramaniam, A. and Zehr, J. P.: Distribution and activity of diazotrophs in the Eastern
527 Equatorial Atlantic, *Environ. Microbiol.*, 11(4), 741–750, doi:10.1111/j.1462-2920.2008.01796.x, 2009.
- 528 Franz, J. M. S., Hauss, H., Sommer, U., Dittmar, T. and Riebesell, U.: Production, partitioning and
529 stoichiometry of organic matter under variable nutrient supply during mesocosm experiments in the
530 tropical Pacific and Atlantic Ocean, *Biogeosciences*, 9(11), 4629–4643, doi:10.5194/bg-9-4629-2012,
531 2012.
- 532 Gao, Y., Kaufman, Y. J., Tanre, D., Kolber, D. and Falkowski, P. G.: Seasonal distributions of aeolian
533 iron fluxes to the global ocean, *Geophys. Res. Lett.*, 28(1), 29–32, doi:10.1029/2000GL01926, 2001.
- 534 Geider, R. and La Roche, J.: Redfield revisited: variability of C:N:P in marine microalgae and its
535 biochemical basis, *Eur. J. Phycol.*, 37(1), 1–17, doi:10.1017/S0967026201003456, 2002.
- 536 Girault, M., Arakawa, H. and Hashihama, F.: Phosphorus stress of microphytoplankton community in
537 the western subtropical North Pacific, *J. Plankton Res.*, 35(1), 146–157, doi:10.1093/plankt/fbs076,
538 2013.
- 539 Grasshoff, K., Kremling, K. and Ehrhardt, M.: *Methods of Seawater Analysis*, 3rd ed., edited by K.
540 Grasshoff, K. Kremling, and M. Ehrhardt, Wiley-VCH Verlag GmbH, Weinheim, Germany. 1999.
- 541 Graziano, L. M., Geider, R. J., Li, W. and Olaizola, M.: Nitrogen limitation of North Atlantic
542 phytoplankton: Analysis of physiological condition in nutrient enrichment experiments, *Aquat. Microb.
543 Ecol.*, 11(1), 53–64, doi:10.3354/ame011053, 1996.
- 544 Großkopf, T., Mohr, W., Baustian, T., Schunck, H., Gill, D., Kuypers, M. M. M., Lavik, G., Schmitz, R.
545 A., Wallace, D. W. R. and LaRoche, J.: Doubling of marine dinitrogen-fixation rates based on direct
546 measurements, *Nature*, 488(7411), 361–364, doi:10.1038/nature11338, 2012.
- 547 Grover, J. P.: *Resource competition*. Chapman & Hall, London, 1997.
- 548 Hansen, H. P. and Koroleff, F.: Determination of nutrients, in *Methods of Seawater Analysis*, edited by
549 K. Grasshoff, K. Kremling, and M. Ehrhardt, pp. 159–228, Wiley-VCH Verlag GmbH, Weinheim,
550 Germany, 1999.
- 551 Hauss, H., Franz, J.M.S., Hansen, T., Struck, U. and Sommer U.: Relative inputs of upwelled and

- 552 atmospheric nitrogen to the eastern tropical North Atlantic food web: Spatial distribution of $\delta^{15}\text{N}$ in
553 mesozooplankton and relation to dissolved nutrient dynamics. *Deep-Sea Res. I*, 75, 135–145,
554 doi:10.1016/j.dsr.2013.01.010, 2013.
- 555 Hecky, R. E., Campbell, P. and Hendzel, L. L.: The Stoichiometry of Carbon, Nitrogen, and
556 Phosphorus in Particulate Matter of Lakes and Oceans, *Limnol. Oceanogr.*, 38(4), 709–724, 1993.
- 557 Hensen, C., Zabel, M. and Schulz, H. N.: Early Diagenesis at the Benthic Boundary Layer: Oxygen,
558 Nitrogen, and Phosphorus in Marine Sediments, in *Marine Geochemistry*, edited by H. D. Schulz and
559 M. Zabel, pp. 207–240, Springer. 2006.
- 560 Holl, C. M. and Montoya, J. P.: Interactions between nitrate uptake and nitrogen fixation in continuous
561 cultures of the marine diazotroph *Trichodesmium* (Cyanobacteria), *J. Phycol.*, 41(6), 1178–1183,
562 doi:10.1111/j.1529-8817.2005.00146.x, 2005.
- 563 Ingall, E. and Jahnke, R.: Evidence for Enhanced Phosphorus Regeneration From Marine Sediments
564 Overlain by Oxygen Depleted Waters, *Geochim. Cosmochim. Acta*, 58(11), 2571–2575,
565 doi:10.1016/0016-7037(94)90033-7, 1994.
- 566 Jaeschke, A., Abbas, B., Zabel, M., Hopmans, E. C., Schouten, S. and Damste, J. S. S.: Molecular
567 evidence for anaerobic ammonium-oxidizing (anammox) bacteria in continental shelf and slope
568 sediments off northwest Africa, *Limnol. Oceanogr.*, 55(1), 365–376, doi:10.4319/lo.2010.55.1.0365,
569 2010.
- 570 Kalvelage, T., Jensen, M. M., Contreras, S., Revsbech, N. P., Lam, P., Günter, M., LaRoche, J., Lavik,
571 G. and Kuypers, M. M. M.: Oxygen Sensitivity of Anammox and Coupled N-Cycle Processes in
572 Oxygen Minimum Zones, *PLoS ONE*, 6(12), e29299, doi:10.1371/journal.pone.0029299.t003, 2011.
- 573 Karl, D. M. and Letelier, R. M.: Nitrogen fixation-enhanced carbon sequestration in low nitrate, low
574 chlorophyll seascapes, *Mar. Ecol. Prog. Ser.*, 364, 257–268, doi:10.3354/meps07547, 2008.
- 575 Karl, D. M., Church, M. J., Dore, J. E., Letelier, R. M. and Mahaffey, C.: Predictable and efficient
576 carbon sequestration in the North Pacific Ocean supported by symbiotic nitrogen fixation, *PNAS*,
577 109(6), 1842–1849, doi:10.1073/pnas.1120312109, 2012.
- 578 Karstensen, J., Stramma, L. and Visbeck, M.: Oxygen minimum zones in the eastern tropical Atlantic
579 and Pacific oceans, *Progr. Oceanogr.*, 77(4), 331–350, doi:10.1016/j.pocean.2007.05.009, 2008.
- 580 Karstensen, J., Fiedler, B., Schütte, F., Brandt, P., Körtzinger, A., Fischer, G., Zantopp, R., Hahn, J.,
581 Visbeck, M., and Wallace, D.: Open ocean dead zones in the tropical North Atlantic Ocean,
582 *Biogeosciences*, 12(8), 2597–2605, doi:10.5194/bg-12-2597-2015, 2015.
- 583 Klausmeier, C. A., Litchman, E., Daufresne, T. and Levin, S. A.: Optimal nitrogen-to-phosphorus
584 stoichiometry of phytoplankton, *Nature*, 429(6988), 171–174, doi:10.1038/nature02508, 2004.
- 585 Lagus, A.: Species-specific differences in phytoplankton responses to N and P enrichments and the
586 N:P ratio in the Archipelago Sea, northern Baltic Sea, *J. Plankton Res.*, 26(7), 779–798,
587 doi:10.1093/plankt/fbh070, 2004.
- 588 Lam, P., Lavik, G., Jensen, M. M., van de Vossenberg, J., Schmid, M., Woebken, D., Gutiérrez, D.,
589 Amann, R., Jetten, M. S. M. and Kuypers, M. M. M.: Revising the nitrogen cycle in the Peruvian
590 oxygen minimum zone, *PNAS*, 106(12), 4752–4757, doi:10.1073/pnas.0812444106, 2009.
- 591 Langlois, R. J., Huemmer, D. and LaRoche, J.: Abundances and distributions of the dominant nifH
592 phylotypes in the Northern Atlantic Ocean, *Appl. Environ. Microbiol.*, 74(6), 1922–1931,
593 doi:10.1128/AEM.01720-07, 2008.
- 594 Langlois, R. J., LaRoche, J. and Raab, P. A.: Diazotrophic diversity and distribution in the tropical and
595 subtropical Atlantic ocean, *Appl. Environ. Microbiol.*, 71(12), 7910–7919,
596 doi:10.1128/AEM.71.12.7910-7919.2005, 2005.

- 597 Liebig, von, J.: Chemistry in its application to agriculture and physiology, 3rd ed., edited by L. Playfair,
598 John Owen, Cambridge. 1842.
- 599 Loescher, C. R., Großkopf, T., Desai, F. D., Gill, D., Schunck, H., Croot, P. L., Schlosser, C.,
600 Neulinger, S. C., Pinnow, N., Lavik, G., Kuypers, M. M. M., LaRoche, J. and Schmitz, R. A.: Facets of
601 diazotrophy in the oxygen minimum zone waters off Peru, ISME J, 8(11), 2180–2192,
602 doi:10.1038/ismej.2014.71, 2014.
- 603 Löscher, C. R., Kock, A., Könneke, M., LaRoche, J., Bange, H. W. and Schmitz, R. A.: Production of
604 oceanic nitrous oxide by ammonia-oxidizing archaea, Biogeosciences, 9(7), 2419–2429,
605 doi:10.5194/bg-9-2419-2012, 2012.
- 606 Mackey, K. R. M.: Phosphorus cycling in the red tide incubator region of Monterey Bay in response to
607 upwelling, Front. Microbiol., 3(33), 1–14, doi: 10.3389/fmicb.2012.00033, 2012.
- 608 Mahaffey, C., Reynolds, S. and Davis, C. E.: Alkaline phosphatase activity in the subtropical ocean:
609 insights from nutrient, dust and trace metal addition experiments, Front. Mar. Sci., 1(73), 1–13,
610 doi:10.3389/fmars.2014.00073, 2014.
- 611 Martin, P., Dyhrman, S. T., Lomas, M. W., Poulton, N. J. and Van Mooy, B. A. S.: Accumulation and
612 enhanced cycling of polyphosphate by Sargasso Sea plankton in response to low phosphorus, PNAS,
613 111(22), 8089–8094, doi:10.1073/pnas.1321719111, 2014.
- 614 Mills, M. M., Ridame, C., Davey, M., La Roche, J. and Geider, R.: Iron and phosphorus co-limit
615 nitrogen fixation in the eastern tropical North Atlantic, Nature, 429(6989), 292–232, doi:
616 10.1038/nature02550, 2004.
- 617 Mohr, W., Großkopf, T., Wallace, D. W. R. and LaRoche, J.: Methodological Underestimation of
618 Oceanic Nitrogen Fixation Rates, edited by Z. Finkel, PLoS ONE, 5(9), e12583,
619 doi:10.1371/journal.pone.0012583, 2010.
- 620 Monteiro, F. M., Dutkiewicz, S. and Follows, M. J.: Biogeographical controls on the marine nitrogen
621 fixers, Global Biogeochem. Cycles, 25(2), GB2003, doi:10.1029/2010GB003902, 2011.
- 622 Moore, M. C., Mills, M. M., Langlois, R., Milne, A., Achterberg, E. P., La Roche, J. and Geider, R.:
623 Relative influence of nitrogen and phosphorus availability on phytoplankton physiology and
624 productivity in the oligotrophic sub-tropical North Atlantic Ocean, Limnol. Oceanogr., 53(1), 291–305,
625 doi: 10.4319/lo.2008.53.1.0291, 2008.
- 626 Moore, C. M., Mills, M. M., Arrigo, K. R., Berman-Frank, I., Bopp, L., Boyd, P. W., Galbraith, E. D.,
627 Geider, R. J., Guieu, C., Jaccard, S. L., Jickells, T. D., La Roche, J., Lenton, T. M., Mahowald, N. M.,
628 Maranon, E., Marinov, I., Moore, J. K., Nakatsuka, T., Oschlies, A., Saito, M. A., Thingstad, T. F.,
629 Tsuda, A. and Ulloa, O.: Processes and patterns of oceanic nutrient limitation, Nat. Geosci., 6(9), 701–
630 710, doi:10.1038/ngeo1765, 2013.
- 631 Mulholland, M. R. and Capone, D. G.: Stoichiometry of nitrogen and carbon utilization in cultured
632 populations of *Trichodesmium* IMS101: Implications for growth, Limnol. Oceanogr., 46(2), 436–443,
633 doi:10.4319/lo.2001.46.2.0436, 2001.
- 634 Mulholland, M. R., Ohki, K. and Capone, D. G.: Nutrient controls on nitrogen uptake and metabolism
635 by natural populations and cultures of *Trichodesmium* (Cyanobacteria), J. Phycol., 37(6), 1001–1009,
636 doi:10.1046/j.1529-8817.2001.00080.x, 2001.
- 637 Parsons, T. R., Maita, Y. and Lalli, C. M.: A manual of chemical and biological methods for seawater
638 analysis, 1984, Pergamon, Oxford. 1984.
- 639 Pennington, J. T., Mahoney, K. L., Kuwahara, V. S., Kolber, D. D., Calienes, R. and Chavez, F. P.:
640 Primary production in the eastern tropical Pacific: A review, Progr. Oceanog., 69(2-4), 285–317,
641 doi:10.1016/j.pocean.2006.03.012, 2006.
- 642 Quigg, A., Finkel, Z. V., Irwin, A. J., Rosenthal, Y., Ho, T.-Y., Reinfelder, J. R., Schofield, O., Morel, F.

- 643 M. and Falkowski, P. G.: The evolutionary inheritance of elemental stoichiometry in marine
644 phytoplankton, *Nature*, 425(6955), 291–294, doi: 10.1038/nature01953, 2003.
- 645 Redfield, A. C.: The Biological Control of Chemical Factors in the Environment, *American Scientist*,
646 46(3), 205–221, 1958.
- 647 Reynolds, S., Mahaffey, C., Roussenov, V. and Williams, R. G.: Evidence for production and lateral
648 transport of dissolved organic phosphorus in the eastern subtropical North Atlantic, *Global*
649 *Biogeochem. Cycles*, 28(8), 805–824, doi:10.1002/2013GB004801, 2014.
- 650 Riebesell, U., Lee, K. and Nejtgaard, J. C.: Pelagic mesocosms, in: *Guide to best practices for ocean*
651 *acidification research and data reporting*, edited by: Riebesell, U., Fabry, V. J., Hansson, L. and
652 Gattuso, J.-P., Luxembourg: Publications Office of the European Union, 95–112, 2010.
- 653 Ruttenberg, K. C.: Dissolved organic phosphorus production during simulated phytoplankton blooms in
654 a coastal upwelling system, *Front. Microbiol.*, 3(274), 1–12, doi: 10.3389/fmicb.2012.00274 , 2012.
- 655 Ryabenko, E., Kock, A., Bange, H. W., Altabet, M. A. and Wallace, D. W. R.: Contrasting
656 biogeochemistry of nitrogen in the Atlantic and Pacific Oxygen Minimum Zones, *Biogeosciences*, 9(1),
657 203–215, doi:10.5194/bg-9-203-2012, 2012.
- 658 Sandel, V., Kiko, R., Brandt, P., Dengler, M., Stemmann, L., Vandromme, P., Sommer, U. and Hauss,
659 H.: Nitrogen Fuelling of the Pelagic Food Web of the Tropical Atlantic, edited by A. C. Anil, *PLoS ONE*,
660 10(6), e0131258, doi:10.1371/journal.pone.0131258, 2015.
- 661 Sanz-Alférez, S. and del Campo, F. F.: Relationship between nitrogen fixation and nitrate metabolism
662 in the *Nodularia* strains M1 and M2, *Planta*, 194(3), 339–345, 1994.
- 663 Schafstall, J., Dengler, M., Brandt, P. and Bange, H.: Tidal-induced mixing and diapycnal nutrient
664 fluxes in the Mauritanian upwelling region, *J. Geophys. Res.*, 115, C10014,
665 doi:10.1029/2009JC005940, 2010.
- 666 Schelske, C. L. and Sicko-Goad, L.: Effect of Chelated Trace Metals on Phosphorus Uptake and
667 Storage in Natural Assemblages of Lake Michigan Phytoplankton, *Journal of Great Lakes Research*,
668 16(1), 82–89, doi:10.1016/S0380-1330(90)71400-1, 1990.
- 669 Sharp, J. H.: Improved analysis for “particulate” organic carbon and nitrogen from seawater, *Limnol.*
670 *Oceangr.*, 19(6), 984–989, doi:10.4319/lo.1974.19.6.0984, 1974.
- 671 Sohm, J. A. and Capone, D. G.: Phosphorus dynamics of the tropical and subtropical north Atlantic:
672 *Trichodesmium* spp. versus bulk plankton, *Mar. Ecol. Prog. Ser.*, 317, 21–28,
673 doi:10.3354/meps317021, 2006.
- 674 Sohm, J. A., Webb, E. A. and Capone, D. G.: Emerging patterns of marine nitrogen fixation, *Nat. Rev.*
675 *Microbiol.*, 9(7), 499–508, doi:10.1038/nrmicro2594, 2011.
- 676 Stewart, R. I. A., Dossena, M., Bohan, D. A., Jeppesen, E., Kordas, R. L., Ledger, M. E., Meerhoff, M.,
677 Moss, B., Mulder, C., Shurin, J. B., Suttle, B., Thompson, R., Trimmer, M. and Woodward, G.:
678 Mesocosm Experiments as a Tool for Ecological Climate-Change Research, *Adv. Ecol. Res.*, 48, 71–
679 181, 2013.
- 680 Subramaniam, A., Mahaffey, C., Johns, W. and Mahowald, N.: Equatorial upwelling enhances nitrogen
681 fixation in the Atlantic Ocean, *Geophys. Res. Lett.*, 40(9), 1766–1771, doi:10.1002/grl.50250, 2013.
- 682 Trimmer, M. and Nicholls, J. C.: Production of nitrogen gas via anammox and denitrification in intact
683 sediment cores along a continental shelf to slope transect in the North Atlantic, *Limnol. Oceangr.*,
684 54(2), 577–589, doi:10.4319/lo.2009.54.2.0577, 2009.
- 685 Tyrrell, T.: The relative influences of nitrogen and phosphorus on oceanic primary production, *Nature*,
686 400(6744), 525–531, doi:10.1038/22941, 1999.

- 687 Tyrrell, T., Maranon, E., Poulton, A. J., Bowie, A. R., Harbour, D. S. and Woodward, E.: Large-scale
688 latitudinal distribution of *Trichodesmium* spp. in the Atlantic Ocean, *J. Plankton Res.*, 25(4), 405–416,
689 doi:10.1093/plankt/25.4.405, 2003.
- 690 Ward, B. A., Dutkiewicz, S., Moore, C. M. and Follows, M. J.: Iron, phosphorus, and nitrogen supply
691 ratios define the biogeography of nitrogen fixation, *Limnol. Oceanogr.*, 58(6), 2059–2075,
692 doi:10.4319/llo.2013.58.6.2059, 2013.
- 693 Weber, T. and Deutsch, C.: Local versus basin-scale limitation of marine nitrogen fixation, *PNAS*,
694 111(24), 8741–8746, doi:10.1073/pnas.1317193111, 2014.
- 695 Zani, S., Mellon, M. T., Collier, J. L. and Zehr, J. P.: Expression of *nifH* genes in natural microbial
696 assemblages in Lake George, New York, detected by reverse transcriptase PCR, *Appl. Environ.*
697 *Microbiol.*, 66(7), 3119–3124, 10.1128/AEM.66.7.3119-3124.2000, 2000.
- 698 Zehr, J. P. and Turner, P. J.: Nitrogen fixation: Nitrogenase genes and gene expression, *Methods in*
699 *Microbiology*, 30, 271–286, doi:10.1016/S0580-9517(01)30049-1, 2001.

700

701

702 **Tables**

703 Table 1: Primers and Probes used in *nifH* TaqMan qPCR assays.

Target Group	Reverse Primer (5'-3')	Forward Primer (5'-3')	Probe (5'-3')
Filamentous (Fil)	GCAAATCCACCGCAAACAAC	TGGCCGTGGTATTATTACTGCT ATC	AAGGAGCTTATACAGATC A
UCYN-A	TCAGGACCACCGACTCAAC	TAGCTGCAGAAAGAGGAAGT AGAAG	TAATTCCTGGCTATAACA
UCYN-B	TCAGGACCACAGATTCTACACACT GGTATCCTTCAAGTAGTACTTCGTCT	TGCTGAAATGGGTTCTGTTGAA TCTACCCGTTTGATGCTACACA	CGAAGACGTAATGCTC AAACTACCATTCTTCACT
UCYN-C	AGCT AACAATGTAGATTTCTGAGCCTTATT	CTAA	GCAG
GamAO	C	TTATGATGTTCTAGGTGATGTG	TTGCAATGCCTATTCCG TCCGGTGGTCCTGAGCC
Het I (Rich-Rizo)	AATACCACGACCCGCACAAC	CGGTTTCCGTGGTGTACGTT	GTGT TCTGGTGGTCCTGAGCC
Het II (Rich-Hemi)	AATGCCGCGACCAGCACAAC	TGTTACCGTGATGTACGTT	GTGT

704

705 **Figure captions**

706 Figure 1: Experimental design and initial nutrient supply conditions during *varied P* (blue circles) and
707 *varied N* (red diamonds). “Cornerpoints” during *varied P* and *varied N* are depicted as grey circles and
708 white diamonds, respectively. Error bars denote the standard deviation of replicated (n=3) treatments.

709 Figure 2: Temporal development of (A) NO_3^- and NO_2^- , (B) PO_4^{3-} , (C) Chl a, (D) POC, (E) PON and
710 (F) POP within all treatments of both experimental runs. Standard deviations are depicted as shaded
711 error bands.

712 Figure 3: Maximum POC, PON and POP accumulation as a function of the initial supply of NO_3^- , PO_4^{3-}
713 and N/P. Maximum δPOM is defined as peak POM concentration subtracted by the initial (day 1) POM
714 concentration. Treatments in *varied P* are depicted as blue circles; treatments in *varied N* are depicted
715 as red diamonds. Error bars denote the standard deviation of replicated (n=3) treatments. Regression
716 lines (continuous lines) indicate significant linear correlations between the initial nutrient supply and
717 POM accumulation.

718 Figure 4: PON/POP stoichiometry during (A) the exponential growth phase and (B) the stationary
719 growth phase of the experiment. The grey line visualizes the Redfield Ratio. The color code, symbols

720 and lines are the same as in Fig. 3.

721 Figure 5: Temporal development of DOP with standard deviations depicted as shaded error bands.

722 Figure 6: Positive linear correlation between maximum DOP accumulation (defined as peak DOP
723 concentration subtracted by the initial DOP concentration) and initial PO_4^{3-} supply during *varied P*
724 (blue circles) and *varied N* (red diamonds).

725 Figure 7: Mean N_2 fixation rates measured on day 2 and day 8 of both experiments. Because of the
726 high variance between replicates we omitted N_2 fixation rates from un-replicated treatments. Asterisks
727 indicate a significant difference between day 2 and day 8 (t-test). Error bars indicate the standard
728 deviation.

729 Figure 8: Temporal development of transcript abundances for (A) *Richelia-Rhizosolenia* (Het I) and
730 filamentous cyanobacteria related to *Trichodesmium* (Fil). Standard deviations are depicted as shaded
731 error bands.

732 Figure 9: Dynamics of PO_4^{3-} , POP and DOP and N_2 fixation rates in mesocosms during *varied P*.
733 Because of the high variance between replicates we omitted N_2 fixation rates from un-replicated
734 treatments.

Figure 1

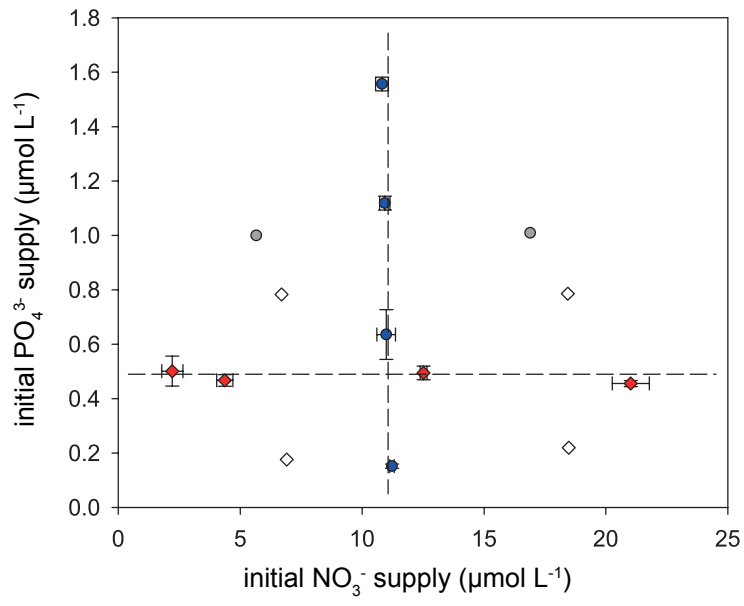


Figure 2

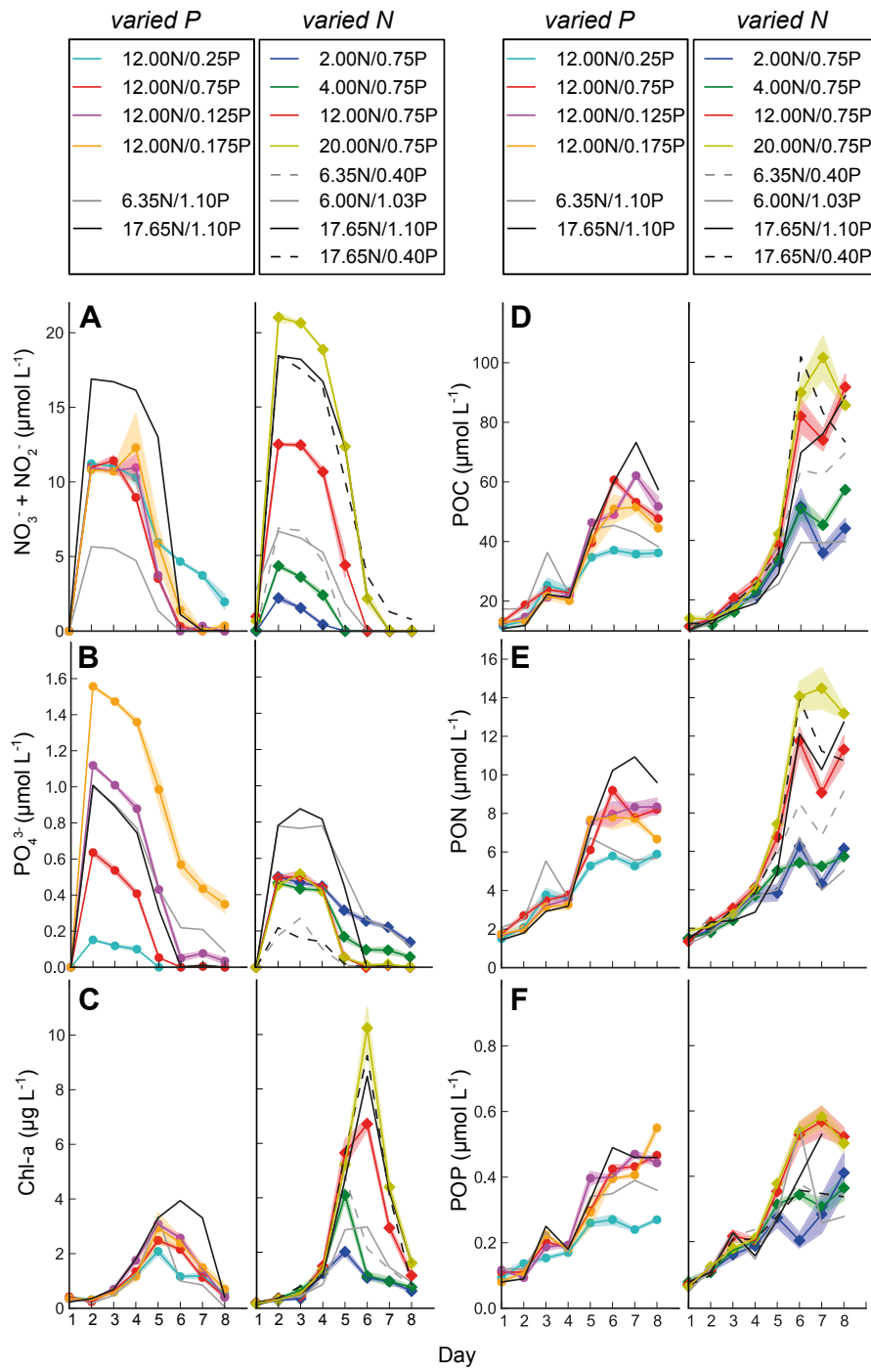


Figure 3

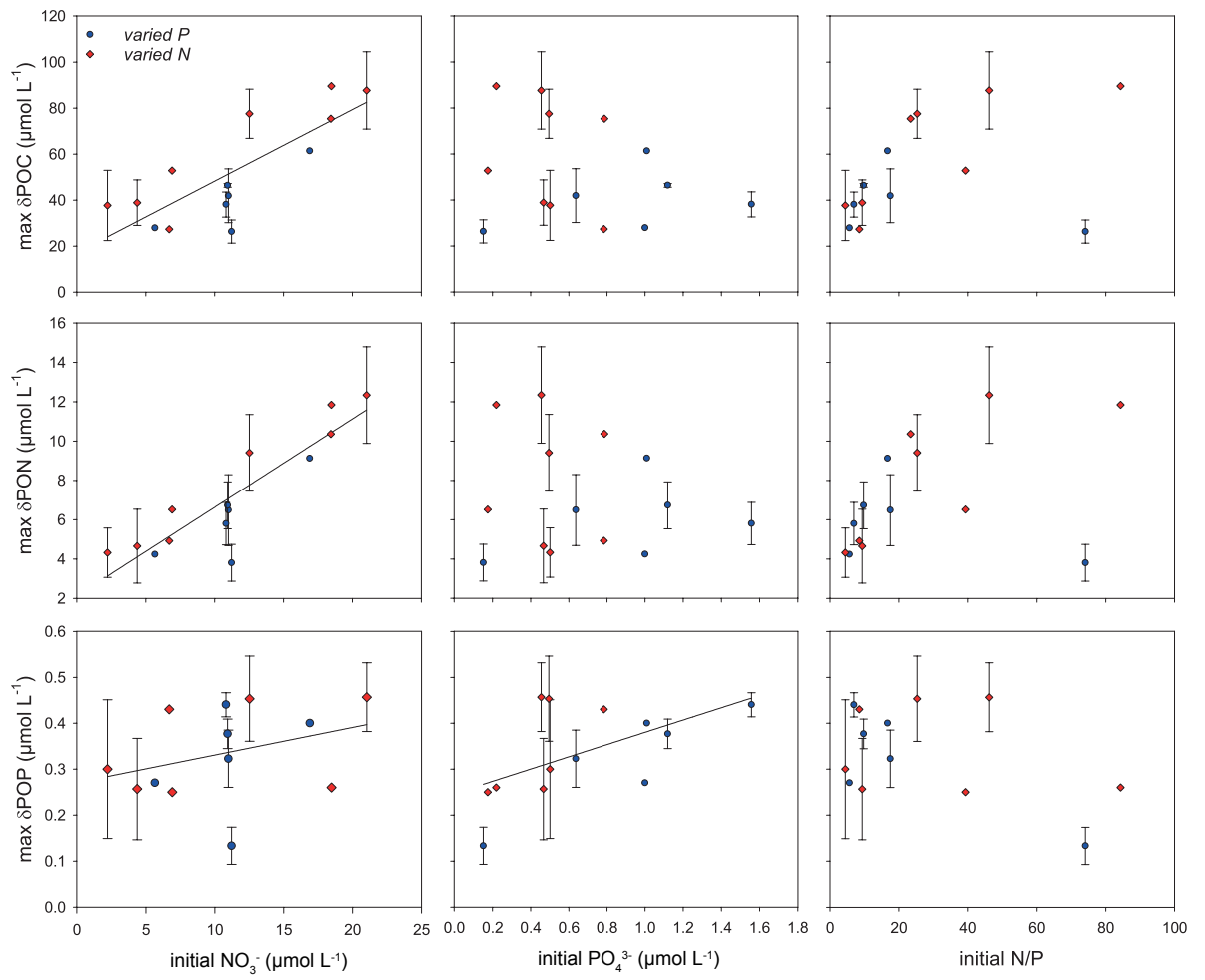


Figure 4

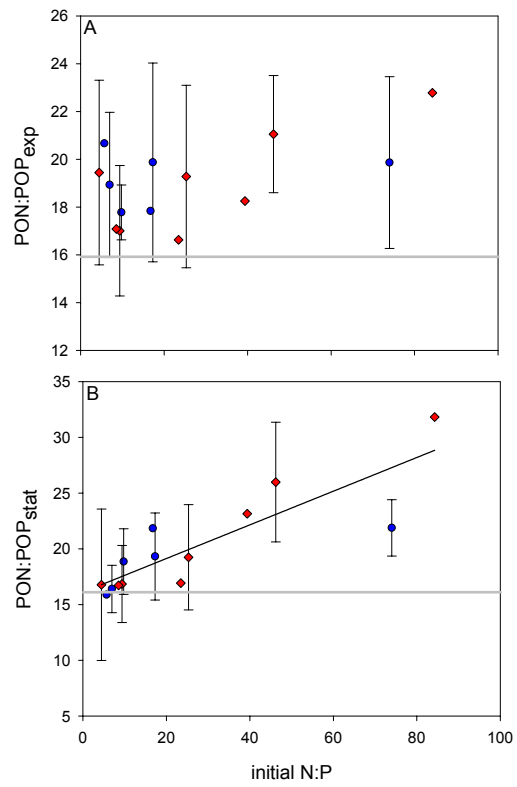


Figure 5

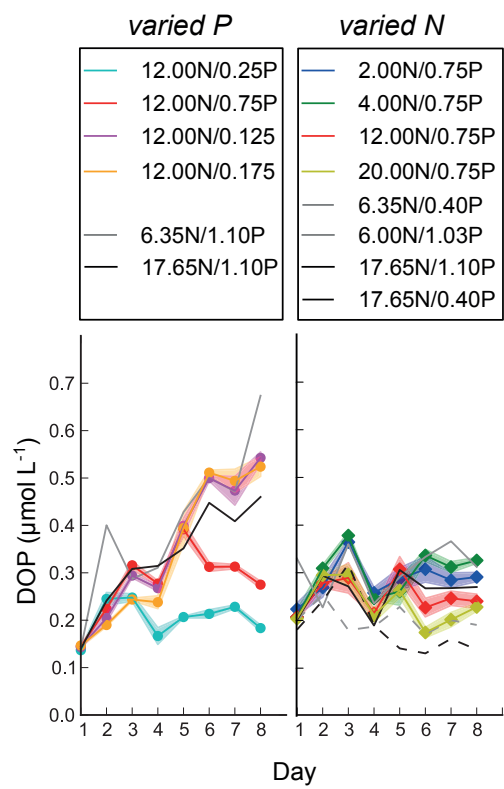


Figure 6

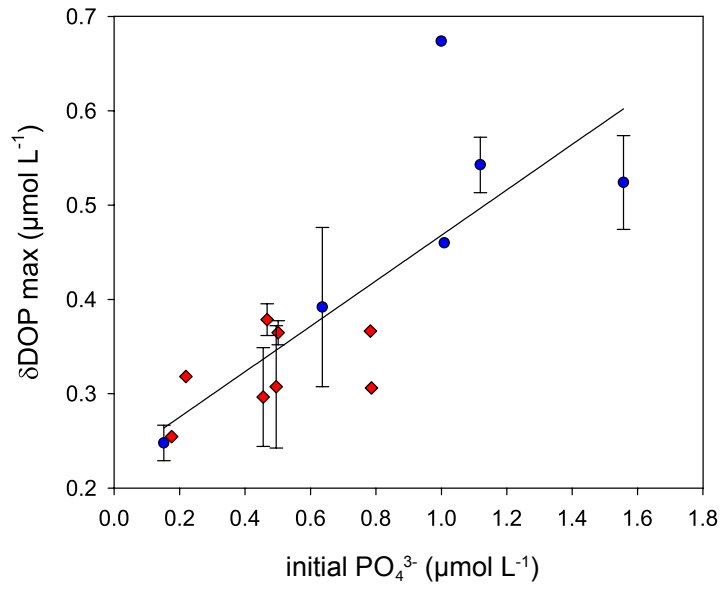


Figure 7

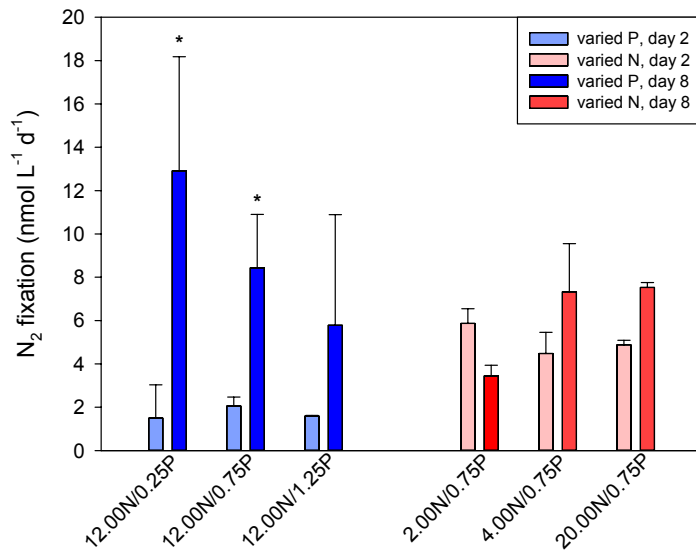


Figure 8

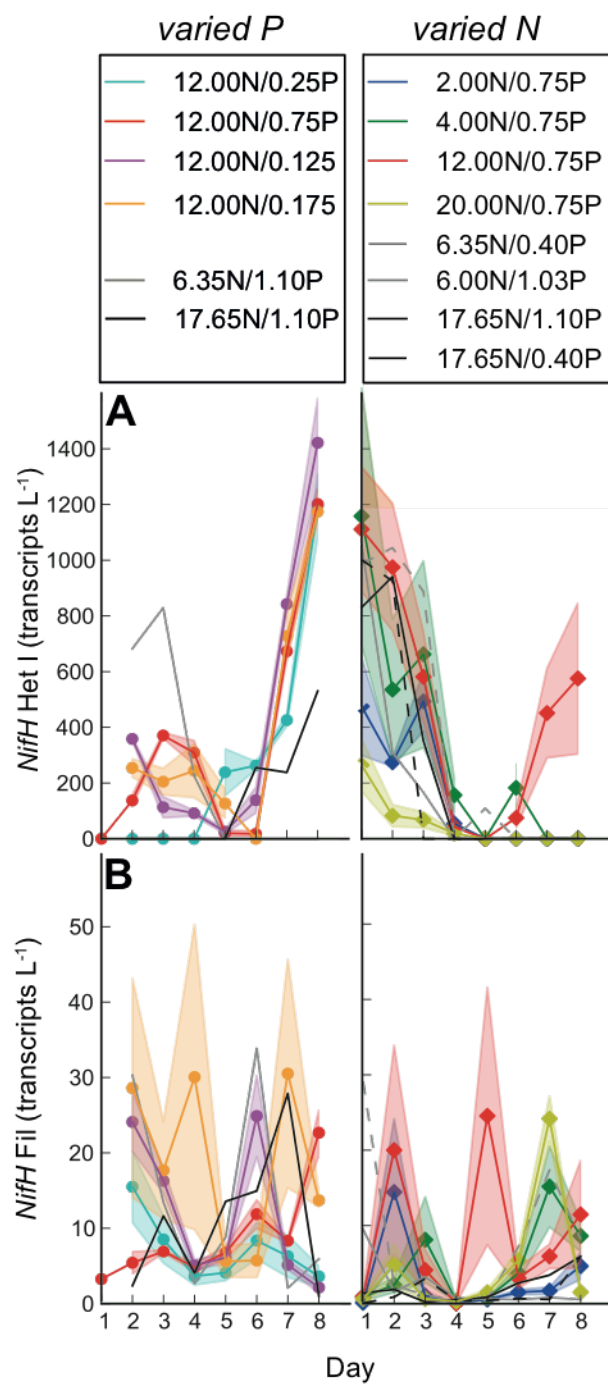


Figure 9

